Improved resistance switching in ZnO-based devices decorated with Ag nanoparticles

2011 J. Phys. D: Appl. Phys. 44 455305

(http://iopscience.iop.org/0022-3727/44/45/455305)

IOP PUBLISHING JOURNAL OF PHYSICS D: APPLIED PHYSICS

J. Phys. D: Appl. Phys. **44** (2011) 455305 (5pp) doi:10.1088/0022-3727/44/45/455305

Improved resistance switching in ZnO-based devices decorated with Ag nanoparticles

L Shi, D S Shang, Y S Chen, J Wang, J R Sun and B G Shen

Beijing National Laboratory for Condensed Matter Physics and Institute of Physics, Chinese Academic of Sciences, Beijing 100190, People's Republic of China

E-mail: jrsun@iphy.ac.cn

Received 11 August 2011, in final form 6 October 2011
Published 28 October 2011
Online at stacks.iop.org/JPhysD/44/455305

Abstract

ZnO is especially attractive among the materials showing resistance switching because of its excellent properties such as light emitting and transparency for visible light. Unfortunately, the resistance switching in a ZnO-based device is usually unstable. By dispersing Ag particles of size ~20 nm at the electrode–ZnO interface, we significantly improved the resistance uniformity, set/reset repeatability of Ag–ZnO–Pt devices. Conducting atomic force microscope analysis revealed the appearance of micro-regions where resistance switching, with an improved stability, is more easily triggered. It is suggested that Ag particles act as seeds for conducting filaments, leading to depressed randomness and reduced diameter of the conducting paths.

(Some figures may appear in colour only in the online journal)

1. Introduction

Electric pulse-triggered resistance switching between different states of metal–oxide–metal structures has attracted considerable attention due to its potential application to nonvolatile memories, known as resistive random access memories (RRAMs) [1–3]. Although RRAMs have many advantages over other technologies of data storage, there are still large obstacles for practical applications. For example, the switching voltage usually distributes in a wide range, and the resistance values of the low-resistance state (LRS) and the high-resistance state (HRS) vary significantly for repeated operations.

The poor stability of an RRAM device could be ascribed to the randomness of the conducting filaments. It has been experimentally revealed that conduction paths across the insulating matrix could be formed under the impact of an electric field, and it is the formation/rupture of these paths that leads to the resistance switching [2, 4]. In general, conduction filaments appear in the form of tree-like structures due to a random dielectric soft breakdown, and distribute irregularly in the oxide for typical RRAM devices. Rearrangements of these paths can occur for repeated writing/easing cycles due to the random ionic migration, which spoils the reversibility and retention of the devices.

To improve the performance of RRAM devices, variant approaches such as impurity doping [5], interface engineering [6] and nanoparticle incorporation have been explored [7]. By introducing Pt particles of appropriate size into TiO_2 films, the distribution of the set/reset voltage has been significantly narrowed [7]; by introducing an interface layer, the resistance behaviour of a LSMO/NSMO/Pt system has been activated [6]; by dispersing Ru particles at the electrode–oxide interface, the resistance uniformity at the reading voltage has been significantly improved [8]. The effects of Au and Pt nanoparticles embedded in the middle of ZrO_2 and TiO_2 oxide films, respectively, have also been studied before [7, 9]. However, the optimization techniques varied from material to material. Seeking effective ways to improve the switching performance more universally is still a great challenge for researchers.

Among the resistance switching materials, ZnO is especially attractive for its several unique advantages, such as the coexisting unipolar and bipolar switching behaviour [10, 11], the larger HRS/LRS window [12], the transparent and flexible application aspects [13, 14]. However, pure ZnO samples always show unstable characteristics and large fluctuations in switching parameters. The impurity doping method has already been adopted to optimize the

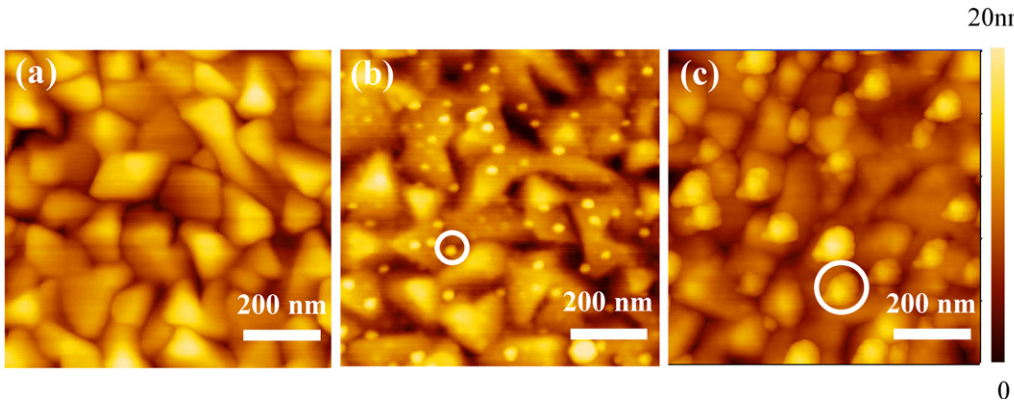

Figure 1. AFM images of the commercial Pt substrate (*a*), the Pt substrate with Ag particles deposited under Ar pressures of 10 Pa (*b*) and 1000 Pa (*c*). Typical Ag particles are marked by circles.

switching performance of ZnO, including Mn, Co, Cu and Ga [11, 12, 15, 16]. In this paper, we present a study of the effects of Ag nanoparticles on the resistance switching of ZnO-based devices. The Ag particles were dispersed on the Pt electrode rather than embedding in the oxide films. This may produce two effects: first, the microstructure of the above ZnO film could be affected; second, the Ag particles may act as extensions of the Pt electrode. By dispersing Ag particles of size ∼20 nm at the electrode–ZnO interface, significantly improved resistance uniformity, set/reset repeatability and retention performance were achieved for the ZnO-based devices. Particularly, the present work further gives a microscopic image of resistance switching with Ag particle decoration. Conducting atomic force microscope (C-AFM) analysis reveals the appearance of micro-regions where resistance switching, with an improved stability, more easily triggered.

2. Experimental

The samples were prepared using the following procedure: Ag particles of different sizes were first deposited on the Pt/Ti/SiO_2/Si substrate by the pulsed laser deposition (PLD) technique from a Ag target of purity 99.99% in an Ar ambient of pressures varied from 10 to 1000 Pa. The target–substrate distance was ∼4 cm. The deposition time was 30 s with a laser energy of 5 J cm^{-2} and a frequency of 10 Hz. After deposition, the chamber was first pumped to 10^{-4} Pa then filled by oxygen of pressure 10 Pa. The ZnO film was afterwards deposited on the Ag-decorated substrate, after replacing the Ag target with a ZnO one without breaking the vacuum. The energy fluence for the laser pulses was 5 J cm^{-2} and the frequency was 2 Hz. The film thickness of ZnO was ∼100 nm, controlled by deposition time (deposition rate = 50 Å min^{-1}). The substrate was kept at room temperature for both deposition processes.

A Rigaku x-ray diffractometer was used to characterize the sample structures. An AFM with its tip coated with Rh was used to analyse the surface morphology and local conductance of the film. For electrical measurements of resistance switching, a top Ag electrode of size 100 × 100 μm^2 was fabricated. The current (I)–voltage (V) characteristics were measured by a Keithley SourceMeter 2612, using a two-probe configuration.

3. Results and discussion

Figure 1 presents the surface morphologies of the Pt substrates, with or without Ag particles. For the commercial Pt substrate, the average grain size is ∼100 nm and the root-mean-square roughness is ∼10 nm for an area of 2 × 2 μm^2. Isolated Ag particles can be clearly seen after the Ag deposition (marked by circles), randomly distributed on the substrate. No preference of the Ag particles to the top or the boundary of the Pt grains is observed. A rough estimation gives a particle density of ∼120 μm^{-2} for the sample prepared under an Ar pressure of 10 Pa. As expected, the particle size strongly depends on Ar pressure, growing from ∼20 to ∼80 nm as the pressure increases from 10 to 1000 Pa. Corresponding to the growth in particle size, particle density decreases.

As will be shown later, the performance of the devices is indeed improved by the incorporation of Ag particles. The optimal particle size is ∼20 nm. Large particles can lead to severe leakage in the resistance switching process. Hereafter we will focus on the 20 nm particle samples. It is also found that the average grain size of the ZnO film is ∼100 nm and the root-mean-square roughness is ∼10 nm (not shown). There are no significant effects of the underlying particles on the morphology of the ZnO film, probably due to the much smaller particle size compared with the film thickness. The presence of Ag does not affect the crystal structure of the ZnO films either. As shown by the x-ray diffraction analysis (figure 2), the ZnO film on Pt is highly textured, and only the (0 0 2) peak can be obtained in the 2θ angle range 30°–60°. It is a result similar to that previously reported [17]. The sharp peak indicates the high quality of the film (figure 2), though the film is prepared at room temperature.

Figure 3(*a*) shows the I–V characteristics of Ag–ZnO–Pt, obtained by repeating the writing–erasing operation for 100 cycles. Typical bipolar resistance switching behaviours were observed. With the increase in applied voltage, the current first grows smoothly then jumps sharply at a critical voltage (set voltage) that is between 0.2 and 2 V, which indicates the resistive transition to the LRS. The device

remains at the LRS in the voltage-decreasing process until a reverse bias of about −0.7 V is applied. After that a switching of the LRS to the HRS occurs and the voltage where the current begins to drop is defined as the reset voltage. Electrical measurements were performed on different locations of the film and different pure ZnO samples, all of which exhibit similar I–V characteristics with large fluctuations in switching parameters. The different I–V curves for repeated switching cycles demonstrate a wide distribution of the set/reset voltage and the LRS/HRS resistance. In contrast, the Ag-decorated devices show a significantly improved switching performance. Figure 3(*b*) illustrates the I–V characteristics of Ag–ZnO/Ag–Pt. The most remarkable observation is the narrowing of the distribution of the set/reset voltages, in addition to the decrease in switching voltage and the improvement of the uniformity of the LRS and HRS resistances. This is a general phenomenon observed in most of the samples studied, ∼60%.

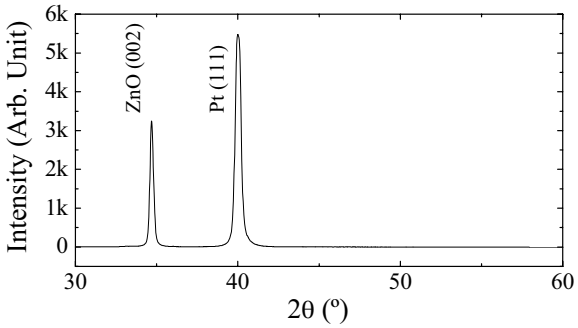

Figure 2. X-ray diffraction pattern of the ZnO_2 film. The film on Pt is highly textured and only the (0 0 2) peak can be seen.

To understand the effect of Ag particles, in figures 3(*c*) and (*d*) we show the statistics of the set/reset voltage and the LRS and HRS resistances, obtained for 100 writing–erasing cycles. For the sample without Ag particles, the critical voltage scatters in a wide range from 0.1 to 2 V for the set operation and from −0.2 to −0.8 V for the reset operation. Meanwhile, the resistance varies from ∼10 to $\sim 10^2$ Ω for the LRS and from $\sim 10^6$ to $\sim 10^8$ Ω for the HRS. In contrast, the switching voltage of the Ag particle-decorated device has a much narrower distribution, from ∼0.1 to ∼0.23 V for the set operation and ∼ − 0.13 to ∼ − 0.23 V for the reset operation. Correspondingly, the LRS resistance locates between ∼10 and ∼20 Ω and the HRS resistance between $\sim 0.8 \times 10^7$ and $\sim 3 \times 10^7$ Ω. A significant improvement of the resistive switching behaviour is clearly demonstrated in the ZnO-based device with Ag particles. Moreover, this phenomenon was also observed in the samples with large Ag particles; however, it leads to large leakage current correspondingly that would affect other characteristics of the device.

Noting the fact that the same programme was used for the electric measurements of the cells with and without Ag nanoparticles, the differences of the two kinds of samples should have a close relation to the Ag particles. To get the microscopic information on how the nanoparticles influence

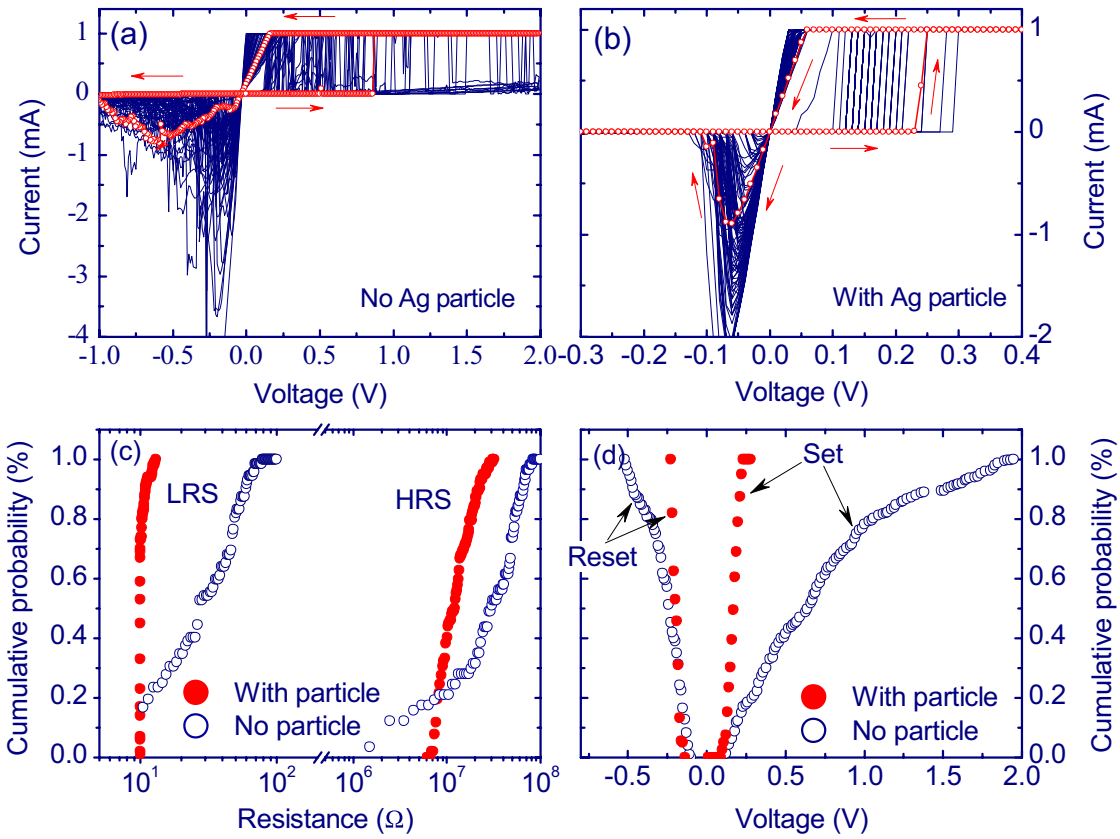

Figure 3. Current–voltage characteristics of the sample without (*a*) and with (*b*) Ag particles (particle size = 20 nm). Two typical I–V cycles, following the directions indicated by arrows, are marked by symbols. (*c*) and (*d*) show the cumulative probability of the LRS/HRS resistances and the set/reset voltages, respectively.

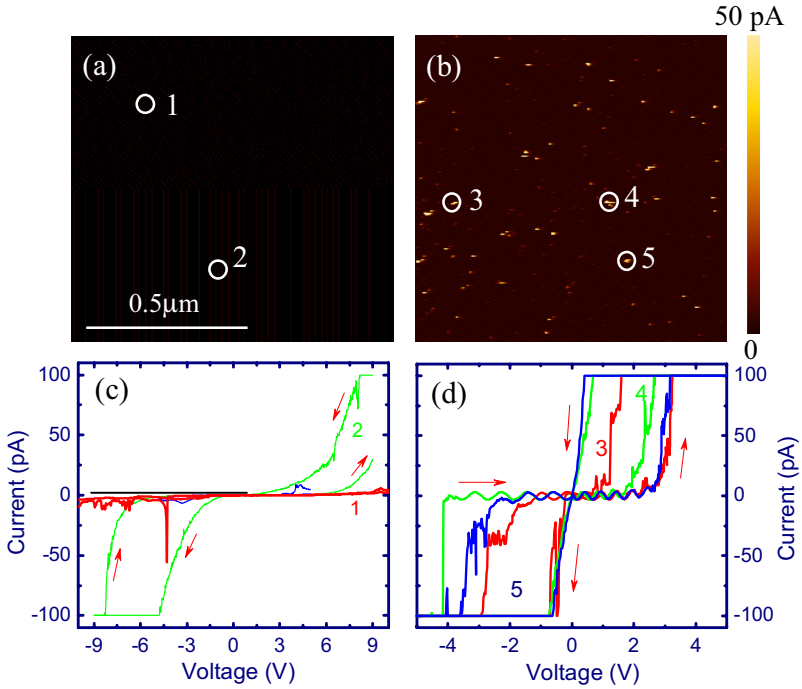

Figure 4. Current mappings of the sample without (*a*) and with (*b*) Ag particles (particle size = 20 nm), measured under a tip bias of 0.5 V. (*c*) and (*d*) show the local I–V characteristics recorded at the spots marked by circles. Arrows indicate the direction for the I–V cycling.

device performance, local resistance switching was further studied. Figure 4 shows the current mapping of the samples without (*a*) and with (*b*) Ag particles, using the bias voltage of 0.5 V by C-AFM (the sample is grounded). The brightness of the image represents the value of current. In the whole area scan, no obvious current peak is observed in the sample without Ag particles, whereas star-like bright spots of size ∼10 nm can be clearly seen in the Ag-decorated sample. This means that the introduction of Ag particles makes the formation of conducting filaments easier. This conclusion is supported by the analysis of the local I–V characteristics. As shown in the bottom panel of figure 4, although hysteretic I–V curves are obtained at different locations of the film, the ones recorded on the bright spot show obviously lower critical voltages and more regular variation for the ascending–descending cycling of the bias voltage.

Usually the top electrode covers a large area of the sample and the switching behaviour detected is an average result. C-AFM can provide the microscopic information of resistance switching. For this purpose, an area of 1 μm × 1 μm on the sample surface was selected, and scanned by the tip biased with −4 V to get a background without any filament spot. To simulate the macroscopic resistance switching, an area of 0.5 μm × 0.5 μm is scanned first with the tip biased by 4 V then with an opposite bias of −4 V, and the current mapping after each scanning is recorded with a lower tip bias (1 V). This process is repeated eight times to trace the evolution of the local resistance. Figure 5 shows the current mappings recorded after the 2, 4, 6 and 8 cycles. For the sample without Ag particles, the number of conducting filaments reduces continuously with the set/reset operations, and most of the conducting filaments become inactive after eight cycles. (This is different from the results of macroscopic measurement, probably due to the large set/reset voltage.) The irregular variation of the filaments can be the reason for the bad switching performance of the device. In contrast, in the sample with Ag particles, the conducting filaments are highly stabilized, and a slight change in filament shapes is observed after repeated set/reset cycles. This result reveals the improvement of the uniformity and endurance of the resistance switching behaviour by the incorporation of Ag particles.

As suggested, the filaments may own a tree-like structure stemming from the electrode due to the random breakdown of the oxides under the applied electric field. Repeated set/reset operations can cause a rearrangement of the tree-like structure in the form of coarsening, bifurcating and merging of the filaments. The Ag particles act as seeds for filament growth, yielding regions that can easily be activated. According to figure 4, the threshold voltage for a resistance switching is generally below 0.5 V in the Ag-decorated samples whereas above 2 V for the film without Ag particles. This implies that as the filaments close and open under the external stimuli, the matrix will remain inactive. As a result, when the density of Ag particles at the interface is so dilute that a cross-linking of different filaments is impossible, the dispersion and rearrangement of the conducing filaments during repeated set/reset cycling will be significantly reduced. This could be the apparent reason for the improvement of the switching characteristics of Ag-decorated devices.

As well documented, interstitial Zn atoms and oxygen vacancies are two mains defects in ZnO, giving rise to n-type carriers [18]. There have been attempts to introduce Ag into ZnO to balance the electron carriers [19]. The Ag atom may not enter the lattice of ZnO because of the low preparing temperature of the present samples, and the associated effects can be ruled out. In fact, the Ag particles dispersing at the

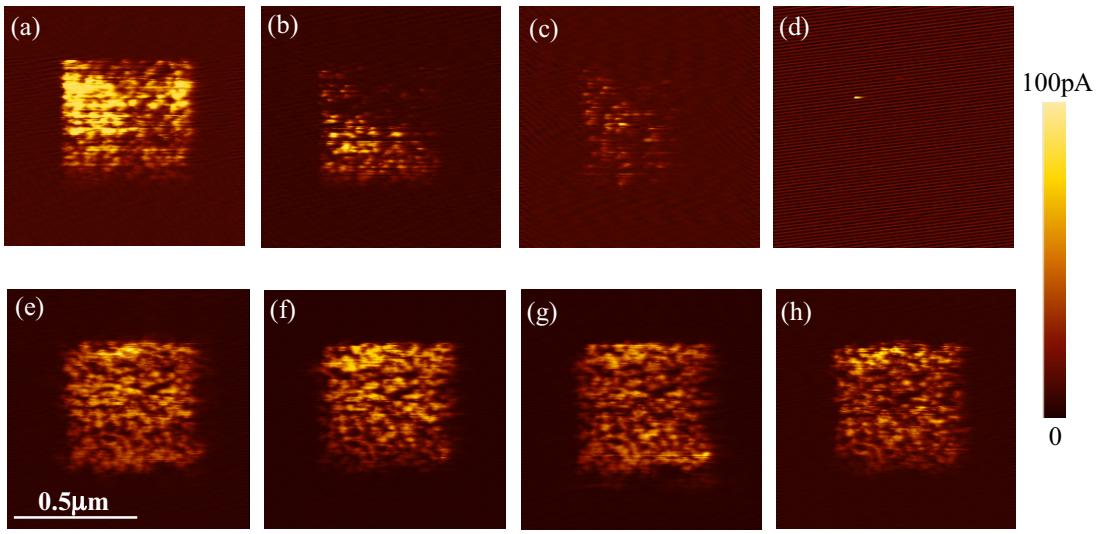

Figure 5. Current mappings of the sample without (top panel) and with (bottom panel) Ag particles (particle size = 20 nm), measured under a tip bias of 1 V. (*a*)/(*e*), (*b*)/(*f*), (*c*)/(*g*), and (*d*)/(*h*) are the results obtained after the 2, 4, 6 and 8 writing operations, respectively.

interface may affect the property of the devices in two manners, either causing the structure defects that lower the breakdown field or migrating into the ZnO matrix under the driving of electric field to give rise to conducting filaments.

The diameter of the conducting filaments may have a close relation to the size of the Ag particles. For the samples with an Ag particle size of ∼20 nm, according to figure 4, the size of the conducting spots formed under the bias of 0.5 V is ∼ 10 nm, quite small. It is the formation and rupture of these filaments that govern the resistance switching of the devices. However, as the size of the Ag particles increases, its effect on ZnO is significantly strengthened. As a consequence, the large leakage current of the ZnO film and the possibility of cross-linking between filaments are enhanced. This has been proved by the results obtained for the samples with Ag particles of 40 and 80 nm. We found that ∼30% and 100% of the corresponding samples are severely leaky, and the resistance switching of the devices has been spoiled.

4. Summary

The resistive switching behaviour of ZnO-based devices was investigated. By dispersing Ag particles of size ∼20 nm at the electrode–ZnO interface, significant improvement of resistance uniformity, set/reset repeatability of the ZnO-based devices is achieved. Conducting AFM analysis reveals the appearance of micro-regions in the Ag-decorated samples, where the resistance switching phenomenon is more easily triggered with an improved stability. It is suggested that the Ag particles act as seeds for the growth of conducting filaments, leading to depressed randomness and reduced diameter of the conducting paths.

Acknowledgments

This work was supported by the National Basic Research of China, the National Natural Science Foundation of China, the Knowledge Innovation Project of the Chinese Academy of Science, the Beijing Municipal Nature Science Foundation.

References

[1] Liu S Q, Wu N J and Ignatiev A 2000 *Appl. Phys. Lett.* **76** 2749
Beck A, Bednorz J G, Gerber Ch, Rossel C and Widmer D 2000 *Appl. Phys. Lett.* **77** 139
[2] Waser R and Aono M 2007 *Nature Mater.* **6** 833
[3] Beck I G *et al* 2005 *Technical Digest IEDM* p 750
Akinaga H and Shima H 2010 *Proc. IEEE* **98** 2237
[4] Waser R, Dittmann R, Staikov G and Szot K 2009 *Adv. Mater.* **21** 2632
[5] Gao B *et al* 2009 *Symp. on VLSI Technology (Kyoto, Japan)* p 30
[6] Sawa A, Fujii T, Kawasaki M and Tokura Y 2006 *Appl. Phys. Lett.* **88** 232112
[7] Chang W-Y, Cheng K-J, Tsai J-M and Chen H-J 2009 *Appl. Phys. Lett.* **95** 042104
[8] Yoon J H, Kim K M, Lee M H, Kim S K, Kim G H, Song S J, Seok J Y and Hwang C S 2010 *Appl. Phys. Lett.* **97** 232904
[9] Guan W, Long S, Jia R and Liu M 2007 *Appl. Phys. Lett.* **91** 062111
[10] Chuang W Y, Lai Y C, Wu T B, Fang S F, Chen F and Tsai M J 2008 *Appl. Phys. Lett.* **92** 022110
[11] Villafuerte M, Heluani S P, Juarez G, Simonelli G, Braunstein G and Duhalde S 2007 *Appl. Phys. Lett.* **90** 052105
[12] Yang Y C, Pan F, Liu Q, Liu M and Zeng F 2009 *Nano Lett.* **9** 1636
[13] Seo J W, Park J W, Lim K S, Yang J H and Kang S J 2008 *Appl. Phys. Lett.* **93** 223505
[14] Lee S, Kim H, Yun D J, Rhee S W and Yong K 2009 *Appl. Phys. Lett.* **95** 262113
[15] Yang Y C, Pan F, Zeng F and Liu M 2009 *J. Appl. Phys.* **106** 123705
[16] Kinoshtia K, Okutani T, Tanaka H, Hinoki T, Yazawa K, Ohmi K and Kishita S 2010 *Appl. Phys. Lett.* **96** 143505
[17] Chen X, Wu G and Hua D 2008 *Appl. Phys. Lett.* **93** 093501
[18] Look D C, Farlow G C, Reunchan P, Limpijumnong S, Zhang S B and Nordlund K 2005 *Phys. Rev. Lett.* **95** 225502
[19] Kang H S, Du Ahn B, Kim J H, Kim G H, Lim S H, Chang H W and Lee S Y 2006 *Appl. Phys. Lett.* **88** 202108